Rv3737 Is Required for Mycobacterium Tuberculosis Growth in Vitro and in Vivo and Correlates With Bacterial Load and Disease Severity in Human Tuberculosis

Qing Li
Affiliated Hospital of Zunyi Medical College
Zhangli Peng
Affiliated Hospital of Zunyi Medical College
Xuefeng Fu
Affiliated Hospital of Zunyi Medical College
Hong Wang
Affiliated Hospital of Zunyi Medical College
Zhaoliang Zhao
Affiliated Hospital of Zunyi Medical College
Yu Pang (pangyupound@163.com)
Beijing Chest Hospital
Ling Chen
Affiliated Hospital of Zunyi Medical College

Research Article

Keywords: Rv3737, Mycobacterium tuberculosis, virulence, transporter

Posted Date: March 5th, 2021

DOI: https://doi.org/10.21203/rs.3.rs-258096/v1

Version of Record: A version of this preprint was published at BMC Infectious Diseases on March 14th, 2022. See the published version at https://doi.org/10.1186/s12879-021-06967-y.

Rv3737 is required for *Mycobacterium tuberculosis* growth *in vitro* and *in vivo* and correlates with bacterial load and disease severity in human tuberculosis

Qing Li, Zhangli Peng, Xuefeng Fu, Hong Wang, Zhaoliang Zhao, Yu Pang, Ling Chen

Abstract

Arms: Rv3737 is the sole homologue of multifunctional transporter ThrE in *Mycobacterium tuberculosis* (*Mtb*). In this study, we aimed to investigate whether this transporter participates *in vitro* and *in vivo* survival of *Mtb*.

Methods: To characterize the role of Rv3737, we constructed and characterized a *Mtb* H37RvΔRv3737. This strain was evaluated for altered growth rate and macrophage survival using a cell model of infection. In addition, the comparative analysis was conducted to determine the association between Rv3737 mRNA expression and disease severity in active pulmonary TB patients.

Results: The H37RvΔRv3737 strain exhibited significantly slow growth rate compared to H37Rv-WT strain in standard culture medium. Additionally, the survival rate of H37Rv-WT strain in macrophages was 2 folds higher than that of H37RvΔRv3737 at 72 h. A significantly higher level of TNF-α and IL-6 mRNA expression was observed in macrophages infected with H37RvΔRv3737 as compared to H37Rv-WT. Of note, Rv3737 expression was significantly increased in clinical *Mtb* isolates than H37Rv-WT. The relative expression level of Rv3737 was positively correlated with lung cavity number of TB patients. Similarly, the higher Rv3737 mRNA level resulted in lower C(t) value by Xpert MTB/RIF assay, demonstrating that a positive correlation between Rv3737 expression and bacterial load in TB patients.

Conclusions: Our data takes the lead in demonstrate that the transporter Rv3737 is required for *in vitro* growth and survival of bacteria inside macrophages. In addition, the expression level of Rv3737 is associated with bacterial load and disease severity in pulmonary tuberculosis patients.

Key Words: Rv3737; Mycobacterium tuberculosis; virulence; transporter

Introduction

Tuberculosis (TB), caused by *Mtb* complex, constitutes a major global health threat. It estimates that one third of the world's population is latently infected by the bacterium, and 10.0 million have fallen ill with TB annually [1]. HIV pandemic and the emergence of multidrug-resistant tuberculosis have contributed further to its spread [2, 3]. The life cycle of *Mtb* involves transition stages from infection, dormancy and reactivation, and active TB is the result of reactivation of latent TB infection in most instances [4]. Specially, individuals with immunosuppression have higher odds of TB reactivation compared with normal individuals [5]. Therefore, *Mtb* is able to survive during periods of reduced growth and has the capacity to regrow rapidly in response to stress encountered in the host.

Bacteria are equipped with a broad variety of transport systems [6]. Transport processes play a pivotal role in pathogen metabolism, e.g. for the uptake of nutrients and excretion of harmful agents [7]. Moreover, several amino acid transporters are indeed reported being associated with pathogenesis [6]. For instance, threonine transporter ThrE is essential for the fitness of *Corynebacterium glutamicum in vitro* growth [8]. Inactivation of *thrE* gene shows reduced growth rate *in vitro* in medium supplemented with threonine. In addition to threonine, the ThrE carrier serves to export small molecules, indicating that it is a multifunctional transporter that gets rid of

metabolic waste products and thus hold more importance to *thrE* in biological fitness [8].

Of note, only two homologues are identified in *Mtb* and *S. coelicolor* [8]. Rv3737 encodes a 55 Da protein with significant sequence similarity to characterized ThrE protein [9]. As a member of new translocator family that has never been reported before, it is interesting to investigate whether this multifunctional potential transporter participates *in vitro* and *in vivo* survival of *Mtb*. To characterize the role of Rv3737, we constructed and characterized an *Mtb* H37RvΔRv3737. This strain was evaluated for altered growth rate and macrophage survival using a cell model of infection. In addition, the comparative analysis was conducted to determine the association between Rv3737 mRNA expression and disease severity in active pulmonary TB patients.

Materials and Methods

Bacterial strains, plasmids and cells

The bacterial strains, plasmids and cells used in this study are detailed in Table S1. *E. coli* DH5α and *E. coli* HB101 cells were grown in Luria-Bertani (LB) broth or LB agar plates at 37°C. Clinical isolates of *Mtb*, *Mtb* reference strain H37Rv (H37Rv-WT, ATCC27294) and *Mycobacterium smegmatis* mc^2 155 cells growth on Lowenstein–Jensen (L-J) medium (Encode, Zhuhai, China), Middlebrook 7H9 broth or 7H10 agar plates containing 0.05% Tween 80, 0.5% glycerol and 10% OADC. The selective 7H9 broth or 7H10 agar plate supplemented with 75 μg/ml hygromycin was used to subculture *Mtb* Rv3737 knockout strain (H37RvΔRv3737). The bacteria with OD_{600} of 0.6-1.0 were used for *in vitro* experiments. RAW264.7 cultured in DMEM complete medium containing 10% Fetal Bovine Serum.

In addition, 12 clinical *Mtb* isolates were collected from a set of sputum smear-positive and

GeneXpert MTB-positive specimens from August 2016 to February 2017. The demographic and clinical characteristics were available from electronic medical records. The number of cavities in the lungs is obtained by reading the images of the patient's chest CT examination. This study was subject to approval by the Ethics Committees of the Affiliated Hospital of Zunyi Medical University. All the patients were≥18 years old and provided written informed consent prior to enrolment.

Construction of H37RvΔRv3737

Using genomic DNA of H37Rv-WT as a template, the Rv3737 nucleic acid sequence was derived from Genbank of NCBI (https://www.ncbi.nlm.nih.gov/gene/885794). As shown in Fig. 1A, the primers for the upper and lower arms of the Rv3737 gene and verification primers were designed based on the principle of homologous recombination (Table S2). Flanking regions comprising upstream and downstream regions of the Rv3737 gene were amplified by PCR and cloned into the p0004S plasmid containing a hygromycin resistance cassette, the vector was then ligated into the phAE159 plasmid, which was electroporated into *M. smegmatis*, and the resulting phage was amplified to obtain a high-titer stock. The high-titer phage was utilized to infect H37Rv-WT, which was plated onto selective 7H10 agar plates. Plates were incubated for 4~8 weeks at 37°C, which eventually gave rise to the growth of a small number of H37RvΔRv3737 colonies. Colonies were picked, and PCR and qPCR were used to confirm the presence of the hygromycin-gene flanking region and the absence of the Rv3737 gene (Fig. 1B, 1C) [10, 11].

Growth and colonial morphology of Rv3737 knockout strain

89 H37RvΔRv3737 was inoculated in selective 7H9 broth medium and incubated at 37°C. Optical
90 density at 600 nm (OD600nm) was detected at intervals of 24 h and the growth curves at 37°C
91 were obtained. H37RvΔRv3737 was inoculated in selective 7H10 agar plates. After incubation for
92 3 weeks at 37°C, the colony morphology was recorded with the HP scanner. The H37Rv-WT was
93 used as a control and the same treatment was performed. For scanning electron microscope
94 analysis, the bacteria were collected by centrifugation at 500 rpm for 5 minutes. Then 2.5%
95 glutaraldehyde was added into the pellet for 24 hours for fixation purpose. Followed by treatment
96 with 1% osmic acid and ethanol gradient, the sample were sprayed with gold film and observed in
97 a SU8010 scanning electron microscope (Hitachi, Japan)[12].

98

99 **Survival of Rv3737 knockout strain in RAW 264.7**

100 H37RvΔRv3737 and H37Rv-WT were infected to 5×10^5/well RAW 264.7 cells in 6-well plate at
101 multiplicity of infection (MOI) 10. After 4 h of incubation, all extracellular bacteria were removed
102 gently by washing and intracellular bacteria were harvested. At 24 h and 72 h after infection, both
103 extracellular bacteria released from macrophage lysed in supernatant and intracellular bacteria in
104 intact cell layer were harvested. Bacteria at 4 h, 24 h and 72 h were plated on 7H10 agar plates in
105 triplicate, plates were incubated for 3 weeks at 37°C and CFU (colony forming unit) were counted
106 [13].

107 **Cytokine measurement**

108 Culture supernatants and sediments from *Mtb*-infected RAW 264.7 cells were harvested at 0 h, 4 h,

8 h, 12 h, 24 h post-infection and stored at − 80 °C for cytokine measurement. The concentrations of TNF-α and IL-6 in culture supernatant were detected using an enzyme-linked immunosorbent assay (ELISA) kit according to the manufacturer's instructions (Solarbio, Beijing, China)[14]. The mRNA level of TNF-α and IL-6 in culture sediments were determined using qPCR. In simple terms, the total RNA was extracted with Trizol method according to the instructions of the manufacturers [15]. After treatment with DNaseI (TaKaRa, Dalian, China), the cDNAs were reverse-transcribed from 5 μg of total RNA with the PrimeScript™ II 1st Strand cDNA Synthesis Kit (TaKaRa, Dalian, China). Real time PCR (qPCR) was carried out in triplicates for each sample using TB Green® Premix Ex Taq™ II (TaKaRa, Dalian, China) in the CFX96 touch Real-Time PCR System (Bio-Rad) [16]. Primers for transcriptional level analysis are listed in Table S2. GAPDH were used as the internal control of the respective qPCR experiments.

Rv3737 expression of clinical isolates and H37Rv-WT

The *Mtb* isolates at log phage were lysed by ultrasound and then subjected to RNA extraction. The mRNA level of Rv3737 in clinical isolates and H37Rv-WT was determined using qPCR method as method above. Primers for transcriptional level analysis are listed in Table S2 and SigA were used as the internal control of the respective qPCR experiments.

Sputum collection, bacterial growth and bacterial load measurement in sputum

Sputum specimens were collected for acid-fast staining and GeneXpert MTB/RIF assay (Cepheid,

Sunnyvale, CA, United States). Acid-fast staining microscopy was performed directly on all samples as described previously [17]. One milliliter sputum was mixed with 2 ml sample reagent, and incubated at room temperature for 15 min. Then the decontaminated sample was then added to a test cartridge and loaded onto the Xpert instrument. Results were reported as the cycle threshold (Ct) values that represented the minimal PCR cycles required for detection threshold [18]. The average Ct values of five probes were used to estimate bacterial load after exclusion of any delayed values due to rifampicin resistance [19]. 1.0 mL of sputum specimen with positive results from both tests were treated with N-acetyl-L-cysteine-NaOH-Na citrate (2.00% final concentration). After neutralization and centrifugation, the suspension of the pellet was inoculated on Lowenstein-Jensen (L-J) medium. The visible growth of colonies on L-J medium was identified using conventional biochemical method [13].

Statistical and analysis

GraphPad Prism v7.03 (GraphPad Software, San Diego, California, USA) was used to analyze the data and generate graphs. *t* test was utilized to compare two groups of data, two-way ANOVA was used for three or more groups of data, considering p value<0.05 to be significant. The linear relationships were analysed by the R squared correlation method. Spearman Coefficient was conducted to establish the relationship between the expression level of Rv3737 and the Ct value yielded by Xpert and between the expression level of Rv3737 and the number of cavities.

Results

Role of Rv3737 in the physiology of *Mtb*

At the amino acid level, Rv3737 shared 29.60% sequence identity with ThrE of *C. glutamicum* (Fig.2). We firstly assessed whether inactivation of Rv3737 affects the *in vitro* growth and physiology of *Mtb*. As shown in Fig. 3A, the H37RvΔRv3737 strain exhibited significantly slow growth rate compared to H37Rv-WT strain in standard culture medium. Colony size of H37RvΔRv3737 and H37Rv-WT strain was compared by plating the same dilution on plates after 21 days (Fig. 3B, 3C). The average colony size of H37RvΔRv3737 was 0.38±0.02 μm, which was much smaller than that of H37Rv-WT strain (0.58±0.02 μm, Fig. 3D).

Field emission scanning electron microscopy was conducted to assess cell morphology and length of *Mtb*. Individuals cells from two strains were indistinguishable in morphology characteristics, whereas significant differences were observed in cell lengths. As noted in Fig. 4, the average cell length of the H37Rv-WT and H37RvΔRv3737 were 1.89 ± 0.04 and 1.69 ± 0.05 μm ($p<0.05$), respectively, suggesting that the latter had a shorter cell length. In contrast, the average cell width of H37RvΔRv3737 was 0.41 ± 0.01 μm, which was statistically higher than that of H37Rv-WT strain (0.35 ± 0.01 μm, $p<0.05$).

Survival of H37RvΔRv3737 in macrophages

Mouse macrophages were infected with H37Rv-WT and with H37RvΔRv3737 to determine differences in capacity for intracellular growth. As shown in Fig. 5A, the intracellular survival was assessed at 24 h and 72 h after infection at 4 h as reference. The survival rate of H37Rv-WT strain was 2 folds higher than that of H37RvΔRv3737 at 72 h, respectively. Taken together, these data indicated that Rv3737 had an important role in enhancing the infection capability and intracellular

172 survival of tubercle bacilli.

173

174 **Detection of proinflammatory cytokines in macrophages**

175 To explore the potential role of Rv3737 in modulating the innate immune response, we
176 investigated the levels of cytokines upon infection of RAW264.7 cells with H37Rv-WT and
177 H37RvΔRv3737. A significantly higher level of TNF-α and IL-6 mRNA expression was observed
178 in macrophages infected with H37RvΔRv3737 as compared to H37Rv-WT (Fig. 5B). Detection of
179 cytokines in the culture supernatants of macrophages also supported the elevated secretion of
180 proinflammatory cytokines (TNF-α and IL-6) at increasing time points (Fig. 5C).

181

182 **Relationship between Rv3737 expression and disease severity**

183 Based on the slower *in vivo* growth and increased host proinflammatory cytokine response, we
184 hypothesized that the expression level of Rv3737 correlated with *Mtb* virulence in the host. In
185 order to test this hypothesis, we recruited 12 clinical *Mtb* isolates to determine whether the
186 upregulation of Rv3737 could lead to more severe clinical symptoms. A total of 12 patients
187 infected with diagnosed TB were retrospectively included in our analysis (Table 1). As shown in
188 Fig. 6A, Rv3737 expression was significantly increased in clinical *Mtb* isolates than H37Rv-WT.
189 Of note, the relative expression level of Rv3737 was positively correlated with lung cavity number
190 of TB patients ($r = 0.71$, $p < 0.01$, Fig. 6B). Similarly, the higher Rv3737 mRNA level resulted
191 in lower C(t) value by Xpert MTB/RIF assay, demonstrating that a positive correlation between
192 Rv3737 expression and bacterial load in TB patients ($r = -0.81$, $p < 0.01$, Fig. 6C).

193

Discussion

Transporter systems are commonly considered as a potential tool for delivery of therapeutic agents. Recently experimental studies reveal that several transporters be required for chronic infection and expression of virulence in pathogenic bacteria [20, 21]. In this study, we attempted to understand the possible role of transporter protein Rv3737, which alters *in vitro* growth and intracellular survival of bacteria inside macrophages. Depletion of Rv3737 in *Mtb* resulted in decreased growth rate *in vitro* compared to H37Rv-WT; however, the mutant strain displayed usual rough and dry colonies as control strain, indicating that Rv3737 might be not involved in the cell wall lipid remodeling in *Mtb*. Although the exact characteristics and role of this transporter in growth profile remain unclear, we speculate that the inactivation of Rv3737 might lead to accumulation of metabolic waste products *in vivo* and consequently inhibit their growth. Further studies will be conducted to determine the change in metabolism profile between H37RvΔRv3737 and H37Rv-WT strain, which is essential to elucidate the substrate preference of this transporter.

Experimental evidence from previous studies confirms that highly virulent *Mtb* isolates have faster *in vivo* doubling time [22, 23]. We found that the knockout of Rv3737 had a markedly negative impact on intracellular survival as compared to the control. On one hand, this fact may reflect the declined growth rate of tubercle bacilli in macrophages, as demonstrated *in vitro* observations. On the other hand, the elevated levels of proinflammatory cytokines were noted in the culture supernatant of macrophages infected with H37RvΔRv3737, thus promoting intracellular bacteria clearance in macrophages. Specific mechanism behind this significant correlation is presently unclear. On the basis of its putative transporter function, the molecules exported by Rv3737 into extracellular substance were able to impair host defense against intracellular bacteria via inhibiting

inflammatory response. On the basis of our findings, Rv3737 may participate in modulation of reduced or delayed host proinflammatory cytokine response, which is required for persisting virulence and survival of *Mtb* within host macrophages.

Furthermore, the elevated expression level of Rv3737 was noted in clinical *Mtb* isolates as compared to H37Rv-WT with attenuated virulence. This diversity supports our previous findings that Rv3737 may be involved in virulence of *Mtb*. Notably, a significant positive correlation between Rv3737 expression level and bacterial load in pulmonary TB patients raises the possibility that the isolates with increased expression of Rv3737 are prone to escape clearance by alveolar macrophages, thus leading to greater bacillary multiplication in the host. The high bacterial burden always causes more lung damage and higher mortality [24, 25]. In line with previous observation, we observed that the higher expression of Rv3737 was most likely to result in more cavities among patients affected by pulmonary TB. In view of the strong association between Rv3737 and lung pathology, we speculate that is could be used as a candidate biomarker for predicting the virulence of distinct isolates, and its potential pathogenic effect in host.

We also acknowledged several obvious limitations to the present study. First, despite exhibiting high identity in amino acid sequence with transporter ThrE, the preferential substrates of Rv3737 remains undetermined, which weaken the significance of our explanation. Second, we observed the slower growth rate and shorter length of H37RvΔRv3737; whereas the mutant had larger width than H37Rv-WT control, which may be associated with the remodeling of cytoskeleton to modulate the bacterial growth. However, the reason for this phenomenon remains unclear. Finally, although we recruited active TB cases in our analysis, the diverse courses of TB disease across patients may serve as a major challenge that biases our conclusion.

Conclusions

In conclusion, our data firstly demonstrate that the transporter Rv3737 is required for *in vitro* growth and survival of bacteria inside macrophages. In addition, the expression level of Rv3737 is associated with bacterial load and disease severity in pulmonary tuberculosis patients. Further studies will be conducted to determine the change in metabolism profile between H37RvΔRv3737 and H37Rv-WT strain, which is essential to elucidate the substrate preference of this transporter.

Availability of data and materials

The datasets used and/or analysed during the current study are available from the corresponding author on reasonable request.

Abbreviations

ANOVA: analysis of variance

CFU: colony forming units

cDNA: complementary deoxyribonucleic acid

DMEM: dulbecco's modified eagle medium

ELISA: enzyme-linked immunosorbent assay

GAPDH: glyceraldehyde-3-phosphate dehydrogenase

HIV: human immunodeficiency virus

IL: interleukin

LB: Luria-Bertani

L-J: Lowenstein-Jensen

***Mtb*/MTB**: *Mycobacterium tuberculosis*

MOI: multiplicity of infection

mRNA: messenger ribonucleic acid

OD: optical density

OADC: oleic albumin dextrose catalase

PCR: polymerase chain reaction

qPCR: the real-time reverse transcription polymerase chain reaction

RIF: rifampin

TNF-α: tumor necrosis factor-α

TB: tuberculosis

WT: wide type

Acknowledgments

The author wish to thank Prof. Mei Liu and Prof. Nana Li for collected and processed the clinical isolates. The author wish to thank Prof. Peng Xu for helpful discussions.

Funding

The study was supported by National Natural Science Foundation of China (81760003 and 81960004).

Author information

Qing Li, Zhangli Peng contributed equally to this work.

Email of first authors

Qing Li: liqyf@163.com

Zhangli Peng: pengzhangli1987@163.com

Affiliations:

Tuberculosis Division of Respiratory and Critical Care Medicine, Affiliated Hospital of Zunyi Medical University, No. 149, Dalian Road, Huichuan District, Zunyi City, 563000, Guizhou Province, China

Qing Li, Zhangli Peng, Xuefeng Fu Hong Wang, Zhaoliang Zhao, Ling Chen

National Clinical Laboratory on Tuberculosis, Beijing Key laboratory for Drug Resistant Tuberculosis Research, Beijing Chest Hospital, Capital Medical University, Beijing Tuberculosis and Thoracic Tumor Institute, Area 2, Yard 9, Beiguan Street, Yongzhun Town, Tongzhou District, Beijing, 101100, Beijing, China.

Qing Li, Yu Pang

Author contributions

QL, ZP, LC, and YP designed the experiments. QL, ZP, XF, HW, and ZZ performed the experiment. QL, ZP, LC, and ZP wrote the manuscript. QL, ZP, CL, and YP edited and approved the manuscript.

Corresponding author

Correspondence to Yu Pang, pangyupound@163.com and Ling Chen, Lingjuncd@163.com.

Ethics declarations

Ethics approval and consent to participate

This study was subject to approval by the Ethics Committees of the Affiliated Hospital of Zunyi Medical University. All methods were carried out in accordance with relevant guidelines and regulations.

Consent for publication

Informed consent for publication was obtained from all participants.

Potential conflicts of interest

The authors declare no conflict of interest regarding the publication of this paper.

Reference:

1. World Health Organization. **Global tuberculosis report 2020.** Geneva: World Health Organization; 2020.
2. Gandhi NR, Nunn P, Dheda K, Schaaf HS, Zignol M, van Soolingen D, Jensen P, Bayona J: **Multidrug-resistant and extensively drug-resistant tuberculosis: a threat to global control of tuberculosis**. *Lancet* 2010, **375**(9728):1830-1843.
3. Canetti D, Riccardi N, Martini M, Villa S, Di Biagio A, Codecasa L, Castagna A, Barberis I, Gazzaniga V, Besozzi G: **HIV and tuberculosis: The paradox of dual illnesses and the challenges of their fighting in the history**. *Tuberculosis (Edinb)* 2020, **122**:101921.
4. Cano-Muniz S, Anthony R, Niemann S, Alffenaar JC: **New Approaches and Therapeutic Options for Mycobacterium tuberculosis in a Dormant State**. *Clin Microbiol Rev* 2018, **31**(1).
5. Fowler E, Ghamrawi RI, Ghiam N, Liao W, Wu JJ: **Risk of tuberculosis reactivation during interleukin-17 inhibitor therapy for psoriasis: a systematic review**. *J Eur Acad Dermatol Venereol* 2020, **34**(7):1449-1456.
6. Garai P, Chandra K, Chakravortty D: **Bacterial peptide transporters: Messengers of nutrition to virulence**. *Virulence* 2017, **8**(3):297-309.
7. Burkovski A, Kramer R: **Bacterial amino acid transport proteins: occurrence, functions, and significance for biotechnological applications**. *Appl Microbiol Biotechnol* 2002, **58**(3):265-274.
8. Simic P, Sahm H, Eggeling L: **L-threonine export: use of peptides to identify a new translocator from Corynebacterium glutamicum**. *J Bacteriol* 2001, **183**(18):5317-5324.

9. Cole ST, Brosch R, Parkhill J, Garnier T, Churcher C, Harris D, Gordon SV, Eiglmeier K, Gas S, Barry CE, 3rd *et al*: **Deciphering the biology of Mycobacterium tuberculosis from the complete genome sequence**. *Nature* 1998, **393**(6685):537-544.
10. Bartek IL, Woolhiser LK, Baughn AD, Basaraba RJ, Jacobs WR, Jr., Lenaerts AJ, Voskuil MI: **Mycobacterium tuberculosis Lsr2 is a global transcriptional regulator required for adaptation to changing oxygen levels and virulence**. *mBio* 2014, **5**(3):e01106-01114.
11. Lewis DL, Notey JS, Chandrayan SK, Loder AJ, Lipscomb GL, Adams MW, Kelly RM: **A mutant ('lab strain') of the hyperthermophilic archaeon Pyrococcus furiosus, lacking flagella, has unusual growth physiology**. *Extremophiles* 2015, **19**(2):269-281.
12. Shin SY, Bajpai VK, Kim HR, Kang SC: **Antibacterial activity of eicosapentaenoic acid (EPA) against foodborne and food spoilage microorganisms**. *LWT - Food Science and Technology* 2007, **40**(9):1515-1519.
13. Tram TTB, Nhung HN, Vijay S, Hai HT, Thu DDA, Ha VTN, Dinh TD, Ashton PM, Hanh NT, Phu NH *et al*: **Virulence of Mycobacterium tuberculosis Clinical Isolates Is Associated With Sputum Pre-treatment Bacterial Load, Lineage, Survival in Macrophages, and Cytokine Response**. *Front Cell Infect Microbiol* 2018, **8**:417.
14. Gupta PK, Kulkarni S: **Polysaccharide rich extract (PRE) from Tinospora cordifolia inhibits the intracellular survival of drug resistant strains of Mycobacterium tuberculosis in macrophages by nitric oxide induction**. *Tuberculosis* 2018, **113**:81-90.
15. Franzen O, Arner E, Ferella M, Nilsson D, Respuela P, Carninci P, Hayashizaki Y, Aslund L, Andersson B, Daub CO: **The short non-coding transcriptome of the protozoan parasite Trypanosoma cruzi**. *PLoS Negl Trop Dis* 2011, **5**(8):e1283.
16. Kumari B, Saini V, Kaur J, Kaur J: **Rv2037c, a stress induced conserved hypothetical protein of Mycobacterium tuberculosis, is a phospholipase: Role in cell wall modulation and intracellular survival**. *Int J Biol Macromol* 2020, **153**:817-835.
17. Marais BJ, Brittle W, Painczyk K, Hesseling AC, Beyers N, Wasserman E, van Soolingen D, Warren RM: **Use of light-emitting diode fluorescence microscopy to detect acid-fast bacilli in sputum**. *Clin Infect Dis* 2008, **47**(2):203-207.
18. Blakemore R, Story E, Helb D, Kop J, Banada P, Owens MR, Chakravorty S, Jones M, Alland D: **Evaluation of the analytical performance of the Xpert MTB/RIF assay**. *J Clin Microbiol* 2010, **48**(7):2495-2501.
19. Hai HT, Vinh DN, Thu DDA, Hanh NT, Phu NH, Srinivasan V, Thwaites GE, N TTT: **Comparison of the Mycobacterium tuberculosis molecular bacterial load assay, microscopy and GeneXpert versus liquid culture for viable bacterial load quantification before and after starting pulmonary tuberculosis treatment**. *Tuberculosis (Edinb)* 2019, **119**:101864.
20. Flores-Valdez MA, Morris RP, Laval F, Daffe M, Schoolnik GK: **Mycobacterium tuberculosis modulates its cell surface via an oligopeptide permease (Opp) transport system**. *FASEB J* 2009, **23**(12):4091-4104.
21. Dasgupta A, Sureka K, Mitra D, Saha B, Sanyal S, Das AK, Chakrabarti P, Jackson M, Gicquel B, Kundu M *et al*: **An oligopeptide transporter of Mycobacterium tuberculosis regulates cytokine release and apoptosis of infected macrophages**. *PLoS One* 2010, **5**(8):e12225.
22. Sohn H, Lee KS, Kim SY, Shin DM, Shin SJ, Jo EK, Park JK, Kim HJ: **Induction of cell death in human macrophages by a highly virulent Korean Isolate of Mycobacterium tuberculosis and the virulent strain H37Rv**. *Scand J Immunol* 2009, **69**(1):43-50.

23. Smith I: **Mycobacterium tuberculosis pathogenesis and molecular determinants of virulence**. *Clin Microbiol Rev* 2003, **16**(3):463-496.
24. Ravimohan S, Kornfeld H, Weissman D, Bisson GP: **Tuberculosis and lung damage: from epidemiology to pathophysiology**. *Eur Respir Rev* 2018, **27**(147).
25. Murthy SE, Chatterjee F, Crook A, Dawson R, Mendel C, Murphy ME, Murray SR, Nunn AJ, Phillips PPJ, Singh KP *et al*: **Pretreatment chest x-ray severity and its relation to bacterial burden in smear positive pulmonary tuberculosis**. *BMC Med* 2018, **16**(1):73.

Figure Legends

Figure 1 Figure 1 Construction the Rv3737 knockout Mtb strain.

A. The wildtype Rv3737 was substituted with DNA fragment encoding hygromycin resistance by homologous recombination. B. Verification of the Rv3737 knockout *Mtb* strain by PCR amplification; M: DNA Marker 5000 bps; Lane 2: H37RvΔRv3737 left arm PCR product band; Lane 4: H37RvΔRv3737 right arm PCR product band; H37Rv-WT both arms PCR products have no bands. C. Verification of the Rv3737 knockout *Mtb* strain by qPCR, t test, *p < 0.01.

Figure 2 Sequence alignment of Rv3737 sequences in *Mtb*

Searched the protein database at the National Center for Biotechnology Information for Rv3737 in *Mtb* and ThrE in *C. glutamicum* amino acid sequences. ClustalW software (http://www.clustal.org/) was used to align sequences and reconstruct a phylogenetic tree based on sequence similarities. Shared amino acids are highlighted in red selected for testing in this study.

Figure 3 *In vitro* growth of H37RvΔRv3737

A. Growth curve of H37Rv-WT and H37RvΔRv3737 in 7H9 medium. B. Colonies of H37Rv-WT

405 and H37RvΔRv3737 on 7H10 agar grown for 21 days. C. Diameter of colonies of H37Rv-WT
406 and H37RvΔRv3737 on 7H10 agar. Experiments were performed in triplicates. The difference
407 between the wild type and the mutant was significant by Student's *t* test (*, $p<0.05$; **, $p<0.01$;
408 ***, $p<0.001$).
409
410 **Figure 4 Morphological changes between the H37Rv-WT and H37RvΔRv3737 strains**
411 A-D. Scanning electron microscope photographs of strains. Bacteria were grown in 7H9 medium.
412 E. Length of H37Rv-WT and H37RvΔRv3737. F. Width of H37Rv-WT and H37RvΔRv3737.
413 Each assa3y was performed in triplicate. The difference between the wild type and the mutant was
414 significant by Student's t test (*, $p<0.05$; **, $p<0.01$; ***, $p<0.001$).
415
416 **Figure 5 Survival of H37Rv-WT and H37RvΔRv3737 in macrophages**
417 A. Survival analysis of H37Rv-WT and H37RvΔRv3737 in macrophages. C. The mRNA levels of
418 TNF-α and IL-6 in macrophages infected with H37Rv-WT and H37RvΔRv3737. D.
419 Immunoassays for TNF-α and IL-6 in supernatants collected from macrophages infected with
420 H37Rv-WT and H37RvΔRv3737. Experiments were performed in triplicates. The difference
421 between the wild type and the mutant was significant by Student's *t* test (*, $p<0.05$; **, $p<0.01$;
422 ***, $p<0.001$).
423
424 **Figure 6 Correlation between Rv3737 mRNA level and disease severity**
425 A. Comparison of Rv3737 mRNA levels between H37Rv-WT and clinical isolates. B.
426 Relationship between the expression level of Rv3737 and the C(t) value yielded by Xpert. C.

427 Relationship between the expression level of Rv3737 and the number of cavities. Each assay was
428 performed in triplicate. The difference between the wild type and the mutant was significant by
429 Student's t test (*, $p<0.05$; **, $p<0.01$; ***, $p<0.001$). The relationship between the expression
430 level of Rv3737 and the C(t) value yielded by Xpert and between the expression level of Rv3737
431 and the number of cavities was established by Spearman Coefficient ($p < 0.01$).

Figures

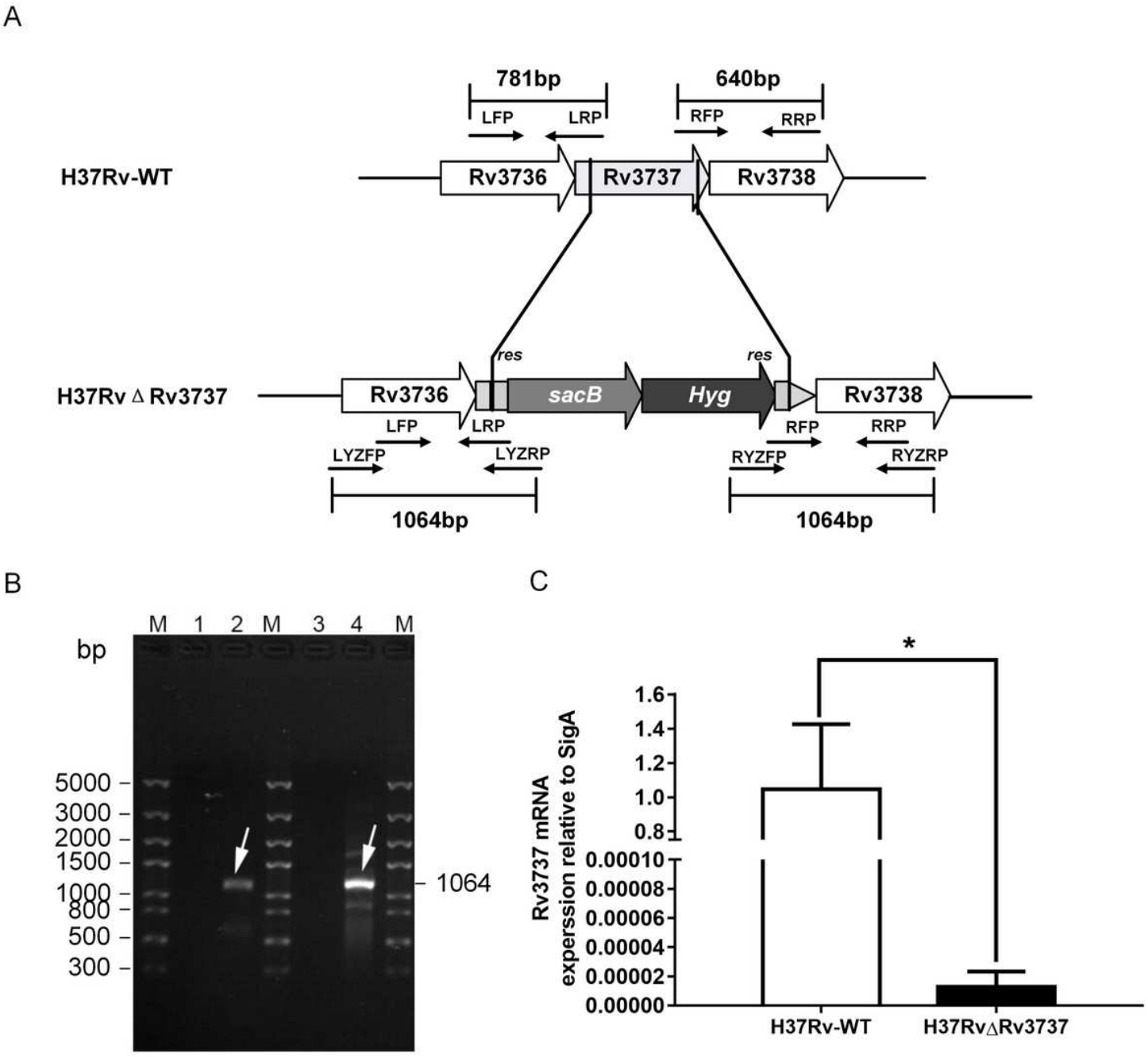

Figure 1

Construction the Rv3737 knockout Mtb strain. A. The wildtype Rv3737 was substituted with DNA fragment encoding hygromycin resistance by homologous recombination. B. Verification of the Rv3737 knockout Mtbstrain by PCR amplification; M: DNA Marker 5000 bps; Lane 2: H37RvΔRv3737 left arm PCR product band; Lane 4: H37RvΔRv3737 right arm PCR product band; H37Rv-WT both arms PCR products have no bands. C. Verification of the Rv3737 knockout Mtbstrain by qPCR, t test, *p < 0.01.

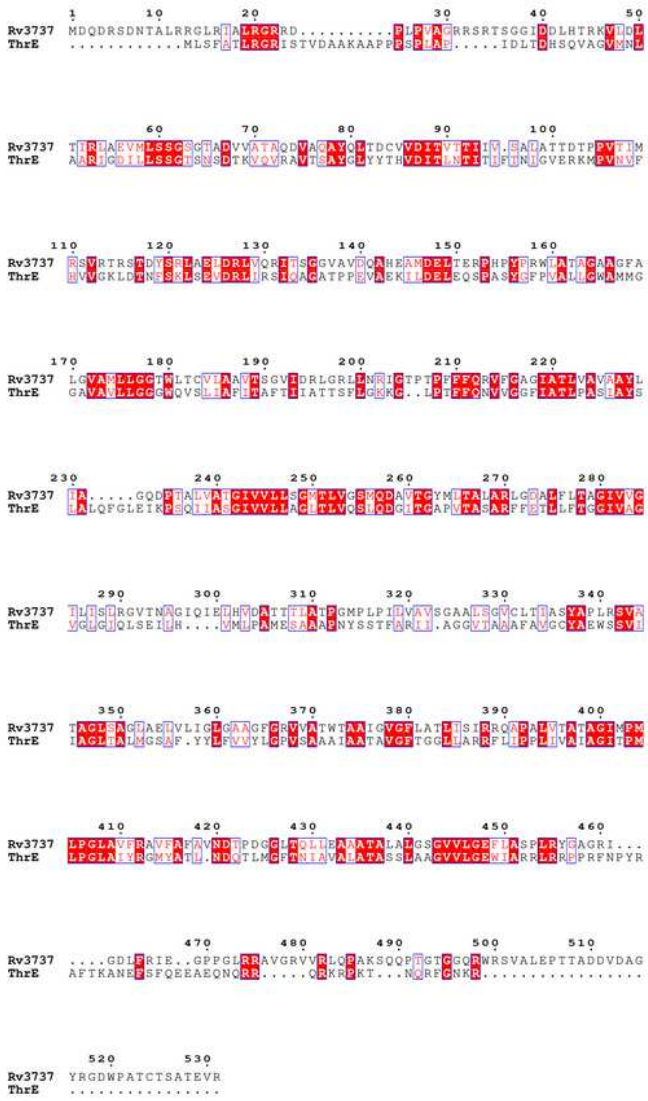

Figure 2

Sequence alignment of Rv3737 sequences in Mtb Searched the protein database at the National Center for Biotechnology Information for Rv3737 in Mtb and ThrE in C. glutamicum amino acid sequences. ClustalW software (http://www.clustal.org/) was used to align sequences and reconstruct a phylogenetic tree based on sequence similarities. Shared amino acids are highlighted in red selected for testing in this study.

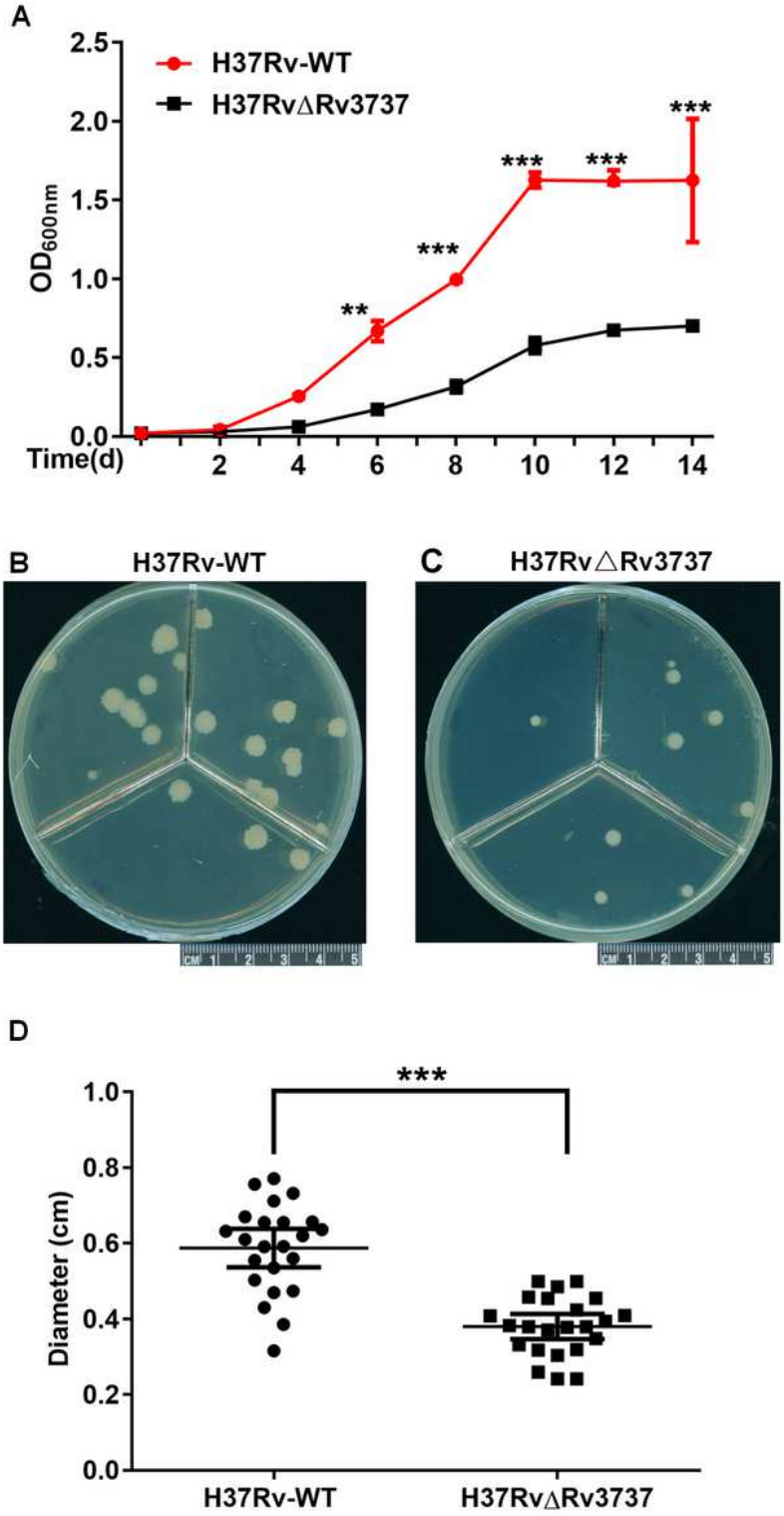

Figure 3

In vitro growth of H37RvΔRv3737 A. Growth curve of H37Rv-WTandH37RvΔRv3737 in 7H9 medium. B. Colonies of H37Rv-WT andH37RvΔRv3737 on 7H10 agar grown for 21 days. C. Diameter of colonies of H37Rv-WT andH37RvΔRv3737 on 7H10 agar.Experiments were performed in triplicates.The difference between the wild type and the mutant was significant by Student's ttest (*,p<0.05; **, p<0.01; ***, p<0.001).

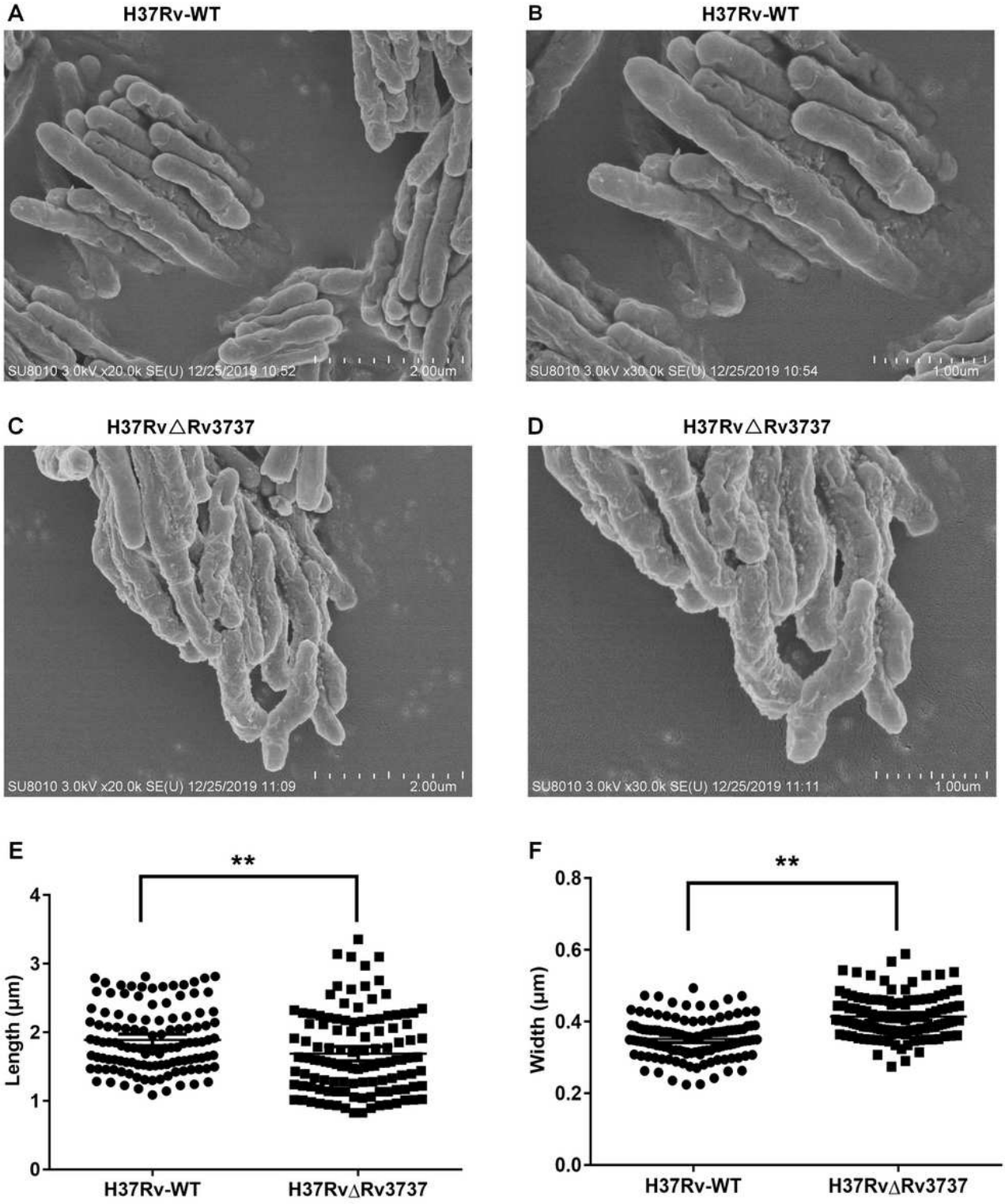

Figure 4

Morphological changes between the H37Rv-WT and H37RvΔRv3737 strains A-D. Scanning electron microscope photographs of strains. Bacteria were grown in 7H9 medium. E. Length of H37Rv-WTandH37RvΔRv3737. F. Width of H37Rv-WTandH37RvΔRv3737. Each assa3y was performed in triplicate.The difference between the wild type and the mutant was significant by Student's t test (*,p<0.05; **, p<0.01; ***, p<0.001).

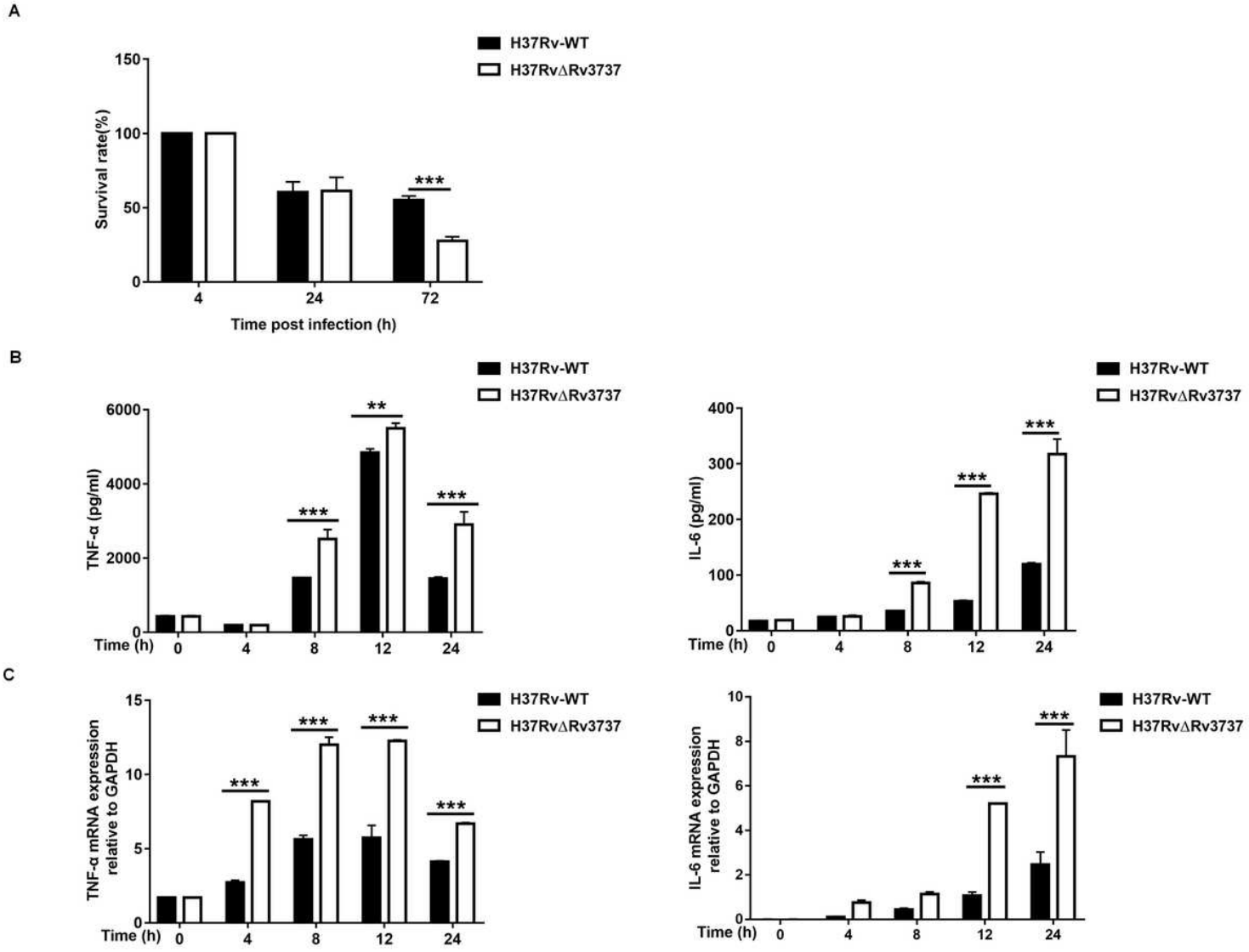

Figure 5

Survival of H37Rv-WTand H37RvΔRv3737in macrophages A.Survival analysis of H37Rv-WTandH37RvΔRv3737in macrophages.C.The mRNA levels of TNF-α and IL-6 in macrophages infected with H37Rv-WTandH37RvΔRv3737. D. Immunoassays for TNF-αand IL-6in supernatants collected from macrophages infected with H37Rv-WTandH37RvΔRv3737. Experiments were performed in triplicates. The difference between the wild type and the mutant wassignificant by Student's ttest (*,$p<0.05$; **, $p<0.01$; ***, $p<0.001$).

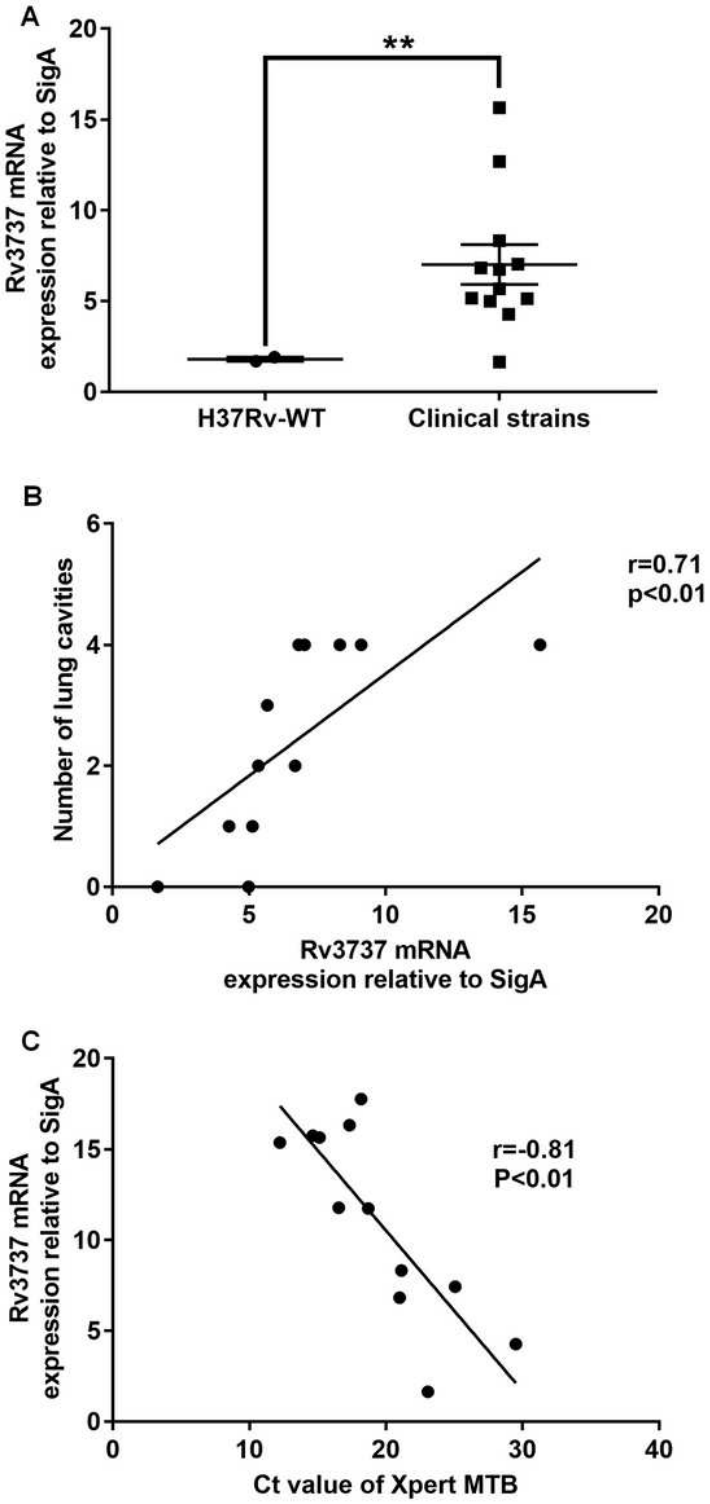

Figure 6

Correlation between Rv3737 mRNA level and disease severity A.Comparison of Rv3737 mRNA levels betweenH37Rv-WTandclinical isolates. B. Relationship between the expression level of Rv3737 and the C(t)value yielded by Xpert. C. Relationship between the expression level of Rv3737 and the number of cavities.Each assay was performed in triplicate.The difference between the wild type and the mutant wassignificant by Student's t test (*,p<0.05; **, p<0.01; ***, p<0.001).The relationship between the

expression level of Rv3737 and the C(t)value yielded by Xpert and between the expression level of Rv3737 and the number of cavitieswas established bySpearman Coefficient($p< 0.01$).

Supplementary Files

This is a list of supplementary files associated with this preprint. Click to download.

- TableS1ofRv3737.docx
- TableS2ofRv3737.docx